Proceedings of the 6th International
Materials Symposium on Ceramic
Microstructures, Berkeley, CA,
August 24 - 27, 1976

LBL-5758
c.1

THE IMPACT OF TRANSMISSION ELECTRON MICROSCOPY IN CERAMICS

Gareth Thomas, David R. Clarke, and
Omer van der Biest

January 1977

Prepared for the U. S. Energy Research and
Development Administration under Contract W-7405-ENG-48

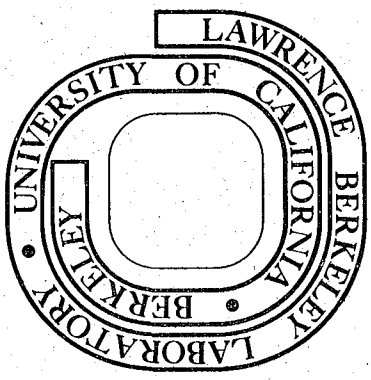

LBL-5758
c.1

THE IMPACT OF TRANSMISSION ELECTRON MICROSCOPY IN CERAMICS

Gareth Thomas, David R. Clarke and Omer van der Biest*
Department of Materials Science and Engineering, College of Engineering and Materials and Molecular Research Division, Lawrence Berkeley Laboratory, University of California, Berkeley, California 94720

ABSTRACT

The impact that transmission microscopy has made in the study of ceramics is illustrated by the following examples from our current work at Berkeley: an absolute structure determination, the study of precipitation and order-disorder phase transformations in lithium ferrite, phase transitions and polytypism in silicon carbide and the investigation of grain boundaries in silicon nitride at lattice resolution, particularly for the presence of amorphous phases.

INTRODUCTION

Transmission electron microscopy has made an impressive impact in ceramics particularly in the ten years that have elapsed since the 1966 Conference here[1]. There are several reasons why this development has occurred in this time period e.g. 1) The problem of preparing samples thin enough for electron transmission has been alievated by advances in techniques, e.g. ion beam thinning[2] and the introduction of high voltage electron microscopes with their greater penetrating power. In 1966 there were no ion thinners or high voltage microscopes in the U.S.A. 2) Many ceramics are beam sensitive, i.e. under electron beam irradiation, damage due to inelastic scattering can destroy the specimen through processes such as ionization. This is far more critical than primary knock-on damage. Since the scattering cross-sections decrease with energy approximately as $(v/c)^3$ (where v is the electron velocity and c is the velocity of light)[3] far less damage occurs to specimens under 1 MeV irradiation compared to say 100 kV (conventional microscopes). This sensitivity to electron beam damage is one of the

* Present Address: EURATOM Research Establishment, Petten, The Netherlands

reasons that MgO has for instance received more attention than the alkali halides[4]. 3) As ceramics generally have complex structures, quantitative microscopy can only be carried out properly when there is adequate theory available for the interpretation of images and diffraction effects. Interest in non-centrosymmetric, anisotropic crystals has now led to the availability of such theories, which can provide detailed structural information directly[5,6,7]. 4) Recently, advances in high resolution electron microscopy have resulted in intensive research efforts in mineralogy and solid state chemistry in which not only can crystal structure analysis be performed directly from images (e.g. Fig. 1), but point defects and their mobility can be observed[7]. As an example, resolutions of better than 1Å were announced just weeks ago by H. Hashimoto[8] who has successfully resolved the atomic arrangements in a [001] gold crystal. Other examples of the application of high resolution electron microscopy to the study of ceramics are given later in this paper.

Most of these developments have been reviewed in recent books (e.g. refs. 9, 10) and electron microscopy conference proceedings, so it is not necessary to review them again here. In addition the application of electron microscopy to ceramics has been so successful that it would be impossible to review all the published work. In this paper, therefore, we shall describe some applications of transmission electron microscopy from current research programs in our group, viz. on ferrites, silicon carbide and silicon nitride, to illustrate the impact that electron microscopy can have. A separate paper deals with defect analysis in ferrites[11].

ABSOLUTE STRUCTURE DETERMINATION

In addition to the crystal structure imaging methods in which the crystal lattice structure is directly imaged, as in Figure 1, contrast experiments and the dynamical theory of electron diffraction can be used to provide structure determination[12]. This technique was developed so as to distinguish the two enantiomorphs co-existing in specimens of ordered lithium ferrite.

In general, when the symmetry operations that constitute the space group of a structure do not include either an inversion or a reflection operation, then the structure can exist in two forms, a right-handed and a left-handed one, known as enantiomorphs. When ordered, lithium ferrite can occur in two enantiomorphic forms, $P4_132$ (having a right-handed screw axis) and $P4_332$ (a left-handed screw axis). The presence of the two enantiomorphs co-existing within a sample can be verified in the electron microscope by imaging in dark field in a many-beam orientation with the electron beam parallel to a zone axis,

along which the crystal does not show a centre of symmetry in projection[13]. Advantage is taken here of violations in Friedel's law[14], which may cause a difference in background intensity between the two structures. An example is shown in Fig. 2, where many inversion boundaries run through a thick crystal of ordered lithium ferrite and where the enantiomorphs can clearly be seen. When imaged in bright field, the enantiomorphs cannot be distinguished. In order to uniquely identify which regions are of which enantiomorph, care must be taken to correctly index the diffraction pattern so as to establish the unique zone axis. An alternative method, which relies on the difference in image intensity profiles for wedge-shaped samples has recently been discussed elsewhere[12].

It should be stressed that whilst the two enantiomorphs possess distinctly different atomic arrangements it is not possible by standard x-ray diffraction techniques to distinguish between the two.

PHASE TRANSITIONS IN FERRITES

We are interested in the ferrites because of their great commercial importance due to their unique magnetic and electronic properties. Both hard and soft ferrites are extensively used in manufacturing microwave device components, computer memory cores and permanent magnets. Ferrimagnetic oxides with the spinel structure form an important class of the ferrites. Conventionally, grain size and porosity have been used for controlling properties in these materials, but it is very likely that heat treatments producing appropriate microstructures could lead to highly desirable properties. Thus, electron microscopy is essential to obtain basic structural information if progress comparable to that made in physical metallurgy is to be made in ceramics. In our continuing program on microstructural characterization in these materials, studies of phase transformations such as ordering and precipitation reactions as well as analysis of defects are being carried out with particular emphasis on lithium ferrite ($LiFe_5O_8$) spinel.

Many of the properties of ferrimagnetic lithium ferrite which are of interest are influenced by the degree of order of the lithium and iron ions in the compound. The most important of these is the DC electrical resistivity which changes by several orders of magnitude upon ordering. Other properties such as the ferrimagnetic resonance line-width, the magnetocrystalline anisotropy constants and, for polycrystalline samples, the squareness of the hysteresis loop are all influenced to a lesser degree by the state of order.

In the disordered state the compound has the inverse spinel structure (space group Fd3m) with a random mixture of Li^{+} and $3Fe^{3+}$ ions on the octahedral sites. Below 750°C the lithium ions and the iron ions on the octahedral sites order and the space group symmetry is lowered to $P4_132$ ($P4_332$). The resulting domain structures, such as in Fig. 3, have been described in detail by Van der Biest and Thomas[13].

The kinetics of this ordering reaction in single crystals have been studied "in-situ" in the high-temperature stage of a high voltage electron microscope.* Annealing in the normal atmosphere of the microscope leads to a reduction of the compound in a way similar to that found for $CoFe_2O_4$[15]. In order to control the stoichiometry of the compound during the ordering reaction, it is necessary to maintain an oxygen atmosphere around the specimen, hence the use of an "environmental" cell is necessary. In this study the environmental cell designed by Swann[16] for the Imperial College, London, high voltage microscope was used. An oxygen pressure of 40 Torr was found to be high enough to prevent rapid reduction of the compound and yet low enough to allow sufficient electron penetration to form adaquate contrast in the images. To study the ordering reaction the specimen was heated above T_c to about 770°C and then cooled as fast as the stage permitted, to temperatures slightly below the ordering temperature. The changes in the microstructure were followed by imaging in dark field using a superlattice reflection and images were recorded with a low light level TV system or video at a speed of 25 frames/sec. Fig. 3 shows a number of frames from an ordering sequence. The ordered domains, which show up bright against the dark background of the disordered phase, nucleate and grow, until they impinge to form anti-phase boundaries. The apparent density of nuclei is much larger in the thicker parts of the foil than in the thin areas near the edge. This implies that the nucleation is homogeneous throughout the specimen volume and does not take place preferentially at its surface. The edge of the foil is also not a preferred nucleation site. From such experiments and the video recordings the nucleation rate as a function of undercooling has been measured, and the results agree with the predicitions of homogeneous nucleation theory. The measured growth rates of the individual domains proved to be constant and when plotted as a function of the undercooling exhibited a maximum, characteristic of a thermally activated interface controlled growth process (Van der Biest and Thomas, in preparation).

The disordering sequence was also followed "in-situ". It was observed that the disordering always started at the anti-phase boundaries which were replaced by a layer of disordered phase. The domains thus subsequently shrank until they disappeared.

* A movie film (16mm-sound) of this work is available.

PRECIPITATION REACTIONS IN $LiFe_5O_8$

In addition to the order-disorder phase transitions at 750°C, lithium ferrite also undergoes a series of precipitation reactions at higher temperatures. This is a common characteristic of many spinel ferrites when held at relatively high temperatures in air and involves a change in stoichiometry due to a loss of oxygen from the structure and a concomitant precipitation of a cation rich phase. This has, for instance, been observed in cobalt ferrite, where a wurtzite phase (CoFe)O precipitates in the spinel phase[17]. In the lithium ferrite, the situation is rather more complicated since at temperatures above 1000°C lithia loss occurs in addition to oxygen loss. This lithia loss phenomenon in fact is one of the major problems in the fabrication of the compound and has up until now limited its widespread utilization. The precipitation reactions studied by HVEM that occur are reported in detail elsewhere[18], but the main features are as follows. At short annealing times in air at 1200°C oxygen loss is faster than is lithia loss and a cation rich phase, lithium ferrate, $LiFeO_2$ forms as small octahedral precipitates dispersed in a spinel matrix (Fig. 4a). The misfit between the two phases is small as both are based on the cubic close packing of oxygen ions; the only difference being in the cation distribution amongst the interstices. At longer annealing times the particles grow so large (~2500Å) that they begin to lose coherency by forming interface dislocations with a Burgers vector parallel to <110> (Fig. 4b). After prolonged annealing the lithia loss equals the oxygen loss near the edge of a specimen or in a thin sample. Scanning electron microscopy shows that the volatilization of the lithia occurs preferentially at {111} planes as in Fig. 5. This lithia loss causes the $LiFeO_2$ particles to re-dissolve leaving behind the interface dislocation network. In a thin sample with a thickness of a few mils, the final microstructure consists of a single spinel phase, but with a high density of dislocations which are the remenants of the intermediate precipitate interface network. In the interior of the bulk samples, however, the two phase microstructure persists. In the later stages of the phase transformation, particles of a glassy phase are observed. These are not part of the Li-Fe-O system, but rather are actually due to the deliberate incorporation of PbO and B_2O_3 in the preparation of the single crystals used in this work. The magnetic hysteresis properties vary with this precipitation sequence as shown in Fig. 4d. The values of H_c vary

with precipitate volume fraction and interface characteristics in an analogous manner to that well known for the yield strength of precipitation strengthened alloys. A dramatic deterioration in magnetic properties occurs due to the lithia loss, whereas the best properties are associated with the presence of a fine dispersion of coherent precipitates of the $LiFeO_2$ phase (Fig.5a). Thus these preliminary structure-property results show promise for the eventual production of controlled magnetic properties by the incorporation of a fine dispersion of a non-magnetic or para-magnetic (e.g. $LiFeO_2$) phase in a magnetic phase.

A NEW STRUCTURAL PHASE TRANSITION IN $MgAl_2O_4$

In addition to the special diffraction effects mentioned above, electron diffraction itself can provide information on structure at much higher resolution than by x-ray diffraction. For example, many spinel ferrites as well as $MgAl_2O_4$ spinel have been known to have Fd3m space group, as originally determined by Sir W. L. Bragg. However, this has been disputed lately[19] and it has been suggested that the space group of the spinel may be $F\bar{4}3m$ one of lower crystallographic symmetry than Fd3m. In-situ electron microscopy and electron diffraction experiments on $MgAl_2O_4$ spinel (Mishra-private communication) show that the space group of $MgAl_2O_4$ is $F\bar{4}3m$ below ~450°C. Reflections with $h + k = 4n + 2$, which are not allowed for the Fd3m space group appear in the diffraction pattern below this temperature, Fig. 6a. At higher temperatures (>450°C), these reflections disappear and the space group becomes Fd3m (Fig. 6b). Structurally such a transformation corresponds to the displacement of the atoms situated at the octahedral symmetry positions in the high temperature phase to off-center positions in the low temperature phase. On the basis of Landau's theory of second order phase transitions, this transformation could be one of either first or second order. The absence of any observable microstructural changes during the $F\bar{4}3m \rightleftarrows Fd3m$ transition suggest that this is in fact a second order phase transition.

PHASE TRANSFORMATION AND POLYTYPISM IN SILICON CARBIDE

We have been investigating the detailed microstructure of a recently developed form of high density silicon carbide that shows considerable promise for high temperature structural applications. The silicon carbide, produced by a process invented by General Electric Company[20,21] in which boron and excess carbon enable pressureless sintering to occur, has a remarkably uniform grain size and is, by x-ray diffraction, composed of a cubic form. However, after the prolonged heating at above about 1800°C in vacuum, exaggerated grain growth occurs and a phase transformation to the hexagonal form occurs.

Our current interest is to characterize this sequence of reactions and to describe the mechanisms of the transformations.

The characterization is however complicated by the fact that silicon carbide displays extensive polytypism[22], so in addition to the basic cubic (β-SiC) and hexagonal (α-SiC) forms there can exist a multitude of possible hexagonal and rhombohedral variants[23]. This can be qualitatively understood from the close packing of nearest neighbor bonded spheres. The crystal structure of silicon carbide may be represented by the close packing of spheres having predominately first neighbor interactions, such that each silicon atom is surrounded by four carbon atoms with a tetrahedral coordination and vice-versa. Any observed structure can then be described, by analogy with the close-packed layer stacking in face-centered-cubic structures, simply by the stacking sequence of the close-packed planes on the three possible stacking positions A,B, and C where any one of the three layers actually represents a sheet of silicon atoms and a parallel sheet of carbon atoms. A consequence of the close packing of spheres having nearest neighbour interactions is that the energy of the assembly does not depend on the stacking sequence, and so would result in the case of silicon carbide, of a structure showing complete disordering in one dimension. In general this disordering is not complete however and the stacking sequences exhibit certain preferred periodicities with unit cells having either hexagonal or rhombohedral symmetry. A particularly good example of polytypes is shown in Fig. 7 where the periodicity is 12.6Å, corresponding to five composite Si-C layers, and the symmetry of the unit cell is deduced to be rhombohedral. The polytype is probably 15R.

It is in the identification of these stacking sequences that the electron microscope becomes indispensable since they can be present on an extremely fine scale. This is the case in the as-sintered General Electric silicon carbide, for although x-ray diffraction indicates that the material is entirely of the cubic form, electron microscopy reveals the presence of numerous regions down to 15.2Å across which have a hexagonal symmetry. These regions are lath shaped, lie parallel to one another on only one of the possible close packed planes and are inside grains that possess an overall cubic symmetry. An example is shown in Fig. 8. This is a [001] oriented grain and the selected area diffraction patterns taken across the grain demonstrate the co-existence of stacking sequences that have cubic, twinned cubic and hexagonal symmetries. These mixed stacking sequences, revealed by electron microscopy, are so complex that they cannot all be unambiguously recognized as being polytypes. However, conventional tilting and contrast experiments in the microscope show that these features are associated with a displacement vector of $\underline{R} = 1/3[111]$ (equivalently $1/6\langle 211\rangle$) since they become invisible when the specimen is tilted to the [112]

pole. An example of such a series of two beam contrast experiments is shown in Fig. 9. Whilst it has not proven possible as yet to determine whether they are produced by deformation or are grown in, they do appear to be either closely spaced stacking faults or micro-twins. From adjacent regions where they are less closely spaced, the formation of a conventional twinned diffraction pattern suggests strongly that they are indeed micro-twins. The intimate relationship between twinning and polytypism in sphalerite crystals has recently been recognized and is described elsewhere (Clarke, in preparation).

The presence of hexagonal regions within the cubic grains of the as-sintered compacts has important implications for the transformation mechanism to the final hexagonal form. For this reason we have been applying direct lattice imaging and the recently developed technique of optical microdiffraction from the lattice image[24] to obtain quantitative information on the distribution of stacking sequences. Preliminary optical microdiffraction measurements have already been reported[25], so only the lattice imaging results will be described here. The lattice fringe technique in the electron microscope makes it possible to observe the stacking of the close packed planes directly. An example of this is given in Fig. 10 where one set of close-packed planes, spacing 2.52Å, can be clearly seen. In addition, the dark and rather diffuse lines delineate the stacking sequences; these are the lines that are usually seen in the lower resolution images such as in Fig. 7. On the figure the probable polytype designations have been marked and the spatial complexity of the transformation becomes apparent since some of the polytypes are only one unit cell wide and are surrounded on either side by un-transformed cubic phase. Obviously, this type of local crystallographic information can only be obtained by using high resolution electron microscopy.

The next step in understanding the transformation is to observe and identify the faults responsible for the conversion from the cubic structure to one of the hexagonal forms. Whilst this remains to be done there are indications that such transformation faults do indeed exist. Fig. 11 shows an interesting example of microsyntaxy between two polytypes, 10H and what may be designated 5(R), (the R in brackets is meant to imply that the symmetry of this stacking sequence with a periodicity of 12.6Å is probably rhombohedral), where there exist faults, F, which locally change the polytype. These faults are quite elusive and it has not so far been possible to unambiguously characterise them.

Another striking feature of the microstructure of silicon carbide is the exaggerated grain growth that occurs on annealing above about 1800°C. The grains grow as long thin tabular forms. The formation of these tabular grains has hitherto been considered to be caused by the transformation to the hexagonal phase and they have been reported as being hexagonal. However, selected area electron diffraction of a number of these grains

shows that the situation is not so simple. They are predominately cubic, but as with the grains of the as-sintered material there exist local regions of high twinning density, extensive polytypism and considerable intergrowth. The selected area electron diffraction also shows that the tabular grains have grown so as to increase the area of the particular close packed plane on which the twinning and polytypism occur.

Since the final microstructure of the silicon carbide consists of long tabular shaped grains of hexagonal structure all the electron microscope observations can be rationalized by assuming that there are essentially two simultaneous processes occurring on heating. Firstly, there is a grain growth process which is unusual in that the growth only occurs on one of the possible close packed planes, and secondly there is the concomitant transformation from cubic stacking to hexagonal stacking by a twinning or faulting mechanism. In this particular form of silicon carbide the crystal structure transformation is slower than the exaggerated grain growth

INVESTIGATION OF GRAIN BOUNDARIES

In many ceramics the properties, particularly the mechanical properties, are determined by their grain boundaries. This is especially true for the creep properties and the loss of high temperature strength. The grain boundary regions are of further importance since most ceramics are formed by either sintering or hot pressing, both of which depend critically on the properties of the grain surfaces and boundaries. Clearly, then, their characterization in ceramics is extremely important and whilst electron microscopy is just beginning to be brought to bear; three ways in which electron microscopy can help have already been identified and applied.

Firstly, clean surfaces and fracture surfaces can be analysed spectroscopically in a microscope, e.g. by scanning auger microscopy. This is beyond the scope of this paper, but

is discussed elsewhere in this conference[26].

Secondly, valuable crystallographic information can be obtained by electron micro-diffraction techniques. In a conventional transmission microscope the area from which diffraction information can be obtained is chiefly limited by spherical aberrations of the imaging lenses, and at 100 kV this area is limited to a 1μm dia. Since the spherical abberation varies with electron wavelength (approximately as λ^2) there is an advantage to using higher voltages e.g. the area is limited to ~0.02μm at 1 MeV. However, modern analytical microscopes in which very fine, intense probes of electrons can be formed on the specimen reduce the area from which diffraction information can be obtained by several orders of magnitude. In these scanning probe transmission microscopes the area is no longer usually limited by spherical aberrations but rather by signal to noise considerations. One example is shown in Fig. 12 which is taken from a mullite sample (courtesy Professor J. A. Pask) using a modified scanning transmission microscope facility at IBM by R. Geiss[27]. In this example micro-diffraction from a region ~20Å diameter across the grain boundary shows no evidence for an amorphous phase between the two grains.

The third microscope technique that enables one to examine the grain boundaries at high resolution is direct lattice imaging of the crystal planes on either side of the boundary. This is a new technique and early results are discussed in the next section.

LATTICE IMAGING OF GRAIN BOUNDARIES IN SILICON NITRIDE

The investigation of the grain boundaries in silicon nitride is of particular importance at the present time because of the intensive effort in the U.S.A., U.K., Germany and Japan, to demonstrate that silicon nitride can truly be a structurally important high temperature material. One of the major problems preventing its application is the rather dramatic decrease in the strength and toughness of the hot pressed form above about 1000°C. This decrease is generally attributed to the presence of a glassy phase, between the individual silicon nitride grains, which at high temperatures rapidly decreases in viscosity with temperature, flows and allows the grains of silicon nitride to slide past one another. Whilst this model is extremely attractive and the available experimental evidence appears to support the model, no direct observation of a glassy phase between the boundaries has been made. We have tackled this problem by imaging directly the crystal lattice planes up to, and on either side of, selected grain boundaries in a 5% MgO hot pressed silicon nitride.[28] The technique used is that of lattice fringe imaging, which has already proven to be extremely valuable in investigating phase transformations in metallic alloys[29,30] and the structure of a variety of minerals[31].

Before presenting lattice images of a number of boundaries it is important to describe how they were selected. The specimen was translated under the electron beam in the diffraction mode until one, or two adjacent, grains were found to be oriented such that the lowest index planes were parallel to the electron beam. This method was adopted since it was not possible to tilt the specimen in the microscope in order to bring a desired crystallographic orientation into the necessary strongly diffracting condition. Further the low index planes were chosen for imaging since the observational conditions are slightly less stringent than for the high index planes.

Figure 13 is of a high angle boundary between two alpha silicon nitride grains, looking almost straight down the boundary plane. The lattice fringes can be followed right up to the boundary from either side demonstrating the absence of any intergranular amorphous layer. A further striking feature of the micrograph is the straightness and smoothness of the boundary plane which suggests that the surface energy of α-silicon nitride is highly anisotropic.

Another high angle boundary between two α- silicon nitride grains is presented in Figure 14. Here again the crystal lattice fringes can be followed right up to the boundary, indicating that any glassy layer present must certainly be less than 3Å thick. As in the previous lattice image the boundary is very straight, with the exception of unit cell high steps in the boundary at the points arrowed. This is a very interesting observation and suggests that the densification during hot pressing might proceed by a ledge migration mechanism. In this micrograph, as in the previous one, it is noticeable that the fringe spacing does not measurably alter in the vicinity of the boundary, implying that the unit cell and the composition do not change appreciably right up to the boundary.

Since these lattice images and those from many other boundaries indicate the absence of any amorphous or glassy layer between two adjacent grains, the problem arises as to where it is in the microstructure. The evidence that a glassy phase does exist is extremely persuasive and perhaps the strongest pieces are the following. Firstly, the commonest sintering aid, magnesium oxide, used to hot press silicon nitride is known to be capable of forming a magnesium calcium silicate with the silica invariably present on the surfaces of the silicon nitride powders used and the calcium impurities also present in the powder[32]. Secondly, internal friction measurements show that there is a viscous component present, which would be sufficient to form a glassy boundary phase perhaps 50-1000Å thick[33]. Thirdly, there is clear evidence from Auger analysis that fracture surfaces contain a glassy layer[34].

Since these pieces of evidence are based on "averaging" methods it is possible that the glassy phase is indeed present but is inhomogenously distributed. In view of the fact that

a glassy phase is frequently observed at the triple points between grains[35] and that these are often commensurate in size with the grains themselves, whilst none is seen between the grains by lattice imaging, it is difficult to escape the conclusion that the amorphous phase lies entirely at the junction of three or more grains.

SUMMARY

By describing some of the applications of electron microscopy in our own work, we have demonstrated the main advantages of studying ceramics by electron microscopy. a) It enables real space structure analysis to be carried out and to distinguish space groups on a very fine scale. Taken in conjunction with image computational techniques it is also possible to identify and distinguish enantiomorphic forms. b) It is the only technique with which to perform quantitative crystal defect analysis in micron-grained sized materials. c) The progress of phase transitions and structural changes can be followed directly by performing in-situ dynamics experiments in the microscope. d) The structure of a material and in particular the grain boundaries can be imaged directly by high resolution lattice imaging.

From these aspects of characterization the microstructure property analyses can be carried out more completely leading to the possibility of advances in design of ceramic microstructures for improved properties and technical applications.

ACKNOWLEDGEMENTS

We would like to express our appreciation to the following people who have kindly supplied us with materials; Dr. C. Johnson and Dr. S. Prochazka of General Electric Corporate Research Labs (SiC), Dr. R. N. Katz of the Army Materials and Mechanics Research Center (Si_3N_4). This work has been supported by both the National Science Foundation through the Division of Materials Research (D.R.C.) and by the United States Energy Research and Development Administration through the Materials and Molecular Research Division of the Lawrence Berkeley Laboratory. We also thank R. K. Mishra for providing us with unpublished results from his Ph.D. thesis research.

REFERENCES

1. "Ceramic Microstructures" edited R. M. Fulrath and J. A. Pask, J. Wiley and Sons, New York, 1968.
2. D. J. Barber, "Thin Foils of Non-metals made for Electron Microscopy by Sputter-etching", J. Mats. Sci, 5, 1-8 (1970).
3. D. G. Howitt, R. M. Glaeser and G. Thomas, "The Energy Dependence of Electron Radiation Damage in l-valine", J. Ultrastruct. Res., 55, 457-461 (1976).
4. for example, J. Washburn, "The Sodium Chloride Structure", in "Electron Microscopy and Strength of Crystals", edited G. Thomas and J. Washburn, J. Wiley-Interscience, New York, 301-332 (1963).
5. J. M. Cowley, "The electron-optical Imaging of Crystal Lattices", Acta Cryst., 12, 367-375 (1959).
6. J. G. Allpress and J. V. Sanders, "The Direct Observation of the Structure of Real Crystals by Lattice Imaging", J. App. Cryst., 6, 165-190 (1973).
7. J. M. Cowley and S. Iijima, "Direct Imaging of crystal Structures", in "Electron Microscopy in Mineralogy", edited H.-R. Wenk, Springer-Verlag, New York (1976), 123-136.
8. H. Hashimoto, Announced at the Electron Microscopy Society of America Conference, Miami, August 8-13th, 1976.
9. "Electron Microscopy and Micro-beam Analysis", edited B. M. Siegel and D. R. Beaman, J. Wiley & Sons, New York, 1975.
10. "Electron Microscopy in Mineralogy", Coordinating Editor, H.-R. Wenk, Springer-Verlag, New York, 1976.
11. R. K. Mishra and G. Thomas, these proceedings.
12. O. Van der Biest, "Absolute Structure Determination Using Electron Microscopy", 34th Ann. Proc. Electron Microscopy Soc. Amer., 484-485 (1976).
13. O. Van der Biest and G. Thomas, "Identification of Enantiomorphism in Crystals by Electron Microscopy", Acta. Cryst., A31, 70-76 (1975).
14. R. Serneels, M. Snykers, P. Delavignette, R. Gevers and S. Amelinckx, "Friedel's Law in Electron Diffraction as Applied to the Study of Domain Structures in non-centrosymmetrical Crystals", Phys. Stat. Sol., 58, 277-292 (1973).
15. L. C. deJonghe and G. Thomas, "High Voltage Electron Microscopy Studies of Phase Transformations in Cobalt Ferrites", Mats. Sci. and Engng., 9, 259-271 (1971).
16. P. R. Swann, "High Voltage Microscope Studies of Environmental Reactions", in "Electron Microscopy and Studies of Materials", edited, G. Thomas, R. M. Fisher and R. M. Fulrath, University of California Press (1972) 878-904.
17. L. C. de Jonghe, Ph.D. Thesis, University of California, UCRL-20369.
18. R. K. Mishra, O. Van der Biest and G. Thomas, submitted to J. Amer. Cer. Soc.

19. L. Hwang, A. H. Heuer, and T. E. Mitchell, "On the Space Group of $MgAl_2O_4$" Phil. Mag., 28, 241-243 (1973).
20. S. Prochazka and P. C. Smith, "Investigation of Ceramics for High Temperature Turbine Vanes", General Electric Report 74CRD040, April 1974.
21. S. Prochazka and R. J. Charles, "Strength and Microstructure of Dense Hot Pressed Silicon Carbide", in "Fracture Mechanics of Ceramics" volume 2, Plenum Publishing Co. (1974).
22. "Polymorphism and Polytypism in Crystal", A. R. Verna and P. Krishna, J. Wiley and Sons, New York (1966).
23. P. T. B. Shaffer, "A Review of the Structure of Silicon Carbide", Acta Cryst., B25, 477-488 (1969).
24. R. Sinclair, R. Gronsky and G. Thomas, "Optical Diffraction From Lattice Images of Alloys", Acta Met., 24, 784-796 (1976).
25. D. R. Clarke and G. Thomas, "An Optical Diffraction Study of the Stacking Sequences in Silicon Carbide", 34th Ann. Proc. Electron Microscopy Soc. Amer., 492-493 (1976).
26. G. Somorjai, these proceedings.
27. R. Geiss, "Rocking Beam Microarea Diffraction Applied to Metallic Thin Films", 34th Ann. Proc. Electron Microscopy Soc. Amer., 396-397 (1976).
28. D. R. Clarke, "Direct Observation of Lattice Planes at Grain Boundaries in Silicon Nitride", in "Nitrogen Ceramics", the proceedings of an Advanced Study Institute. To be published Spring 1977.
29. R. Sinclair, K. Schneider and G. Thomas, "Analysis of Ordering in Cu_3Au Utilizing Lattice Imaging Techniques", Acta Met., 23, 873-883 (1975).
30. R. Gronsky, M. Okada and R. Sinclair, and G. Thomas, "Lattice Imaging of Spinodal Alloys", 33rd Ann. Proc. Electron Microscopy Soc. Amer., 22-23 (1975).
31. "Electron Microscopy in Mineralogy" edited H.-R. Wenk, Springer-Verlag (1976).
32. P. Drew and M. H. Lewis, "The Microstructure of Silicon Nitride Ceramics During Hot-pressing Transformations", J. Mats. Sci., 9, 261-269 (1974).
33. D. R. Mosher, R. Raj and R. Kossowsky, "Measurement of Viscosity of the Grain Boundary Phase in Hot-pressed Silicon Nitride", J. Mats. Sci., 11, 49-53 (1976).
34. B. D. Powell and P. Drew, "The Identification of a Grain-Boundary Phase in Hot Pressed Silicon Nitride by Auger Electron Spectroscopy", J. Mats. Sci., 9, 1867-1870 (1974).
35. D. R. Clarke, in preparation.

FIGURE CAPTIONS

FIG. 1. A comparison of the structure image of beryl with a projection of the structure. (Courtesy of P. R. Buseck and S. Iijima).

FIG. 2. Dark field electron micrograph of ordered lithium ferrite. Domains of one enantiomorph appear dark and domains of the other appear light.

FIG. 3. Part of an ordering sequence in lithium ferrite observed in-situ using an environmental cell in a high voltage microscope. A super-lattice dark field.

FIG. 4. A precipitation sequence in lithium ferrite. Small octahedral precipitates of lithium ferrate first form (a), grow until they lose coherency by forming interfacial dislocations (b), and finally re-dissolve leaving behind the interfacial dislocation network (c). The effect of these microstructural changes on the magnetic hysteresis properties are shown in (d).

FIG. 5. Scanning electron micrograph of lithium ferrite shows that the volatilization of lithia occurs preferentially at {111} planes.

FIG. 6. Electron diffraction patterns of $MgAl_2O_4$ at room temperature (a) and above the transformation temperature at 450°C (b).

FIG. 7. A superlattice fringe image of polytype 15R in silicon carbide illustrating the 12.5Å periodicity corresponding to blocks of five composite Si-C layers.

FIG. 8. A partially transformed $\beta \rightarrow \alpha$ grain of silicon carbide illustrating the co-existence of cubic, twinned and hexagonally stacked regions within the grain.

FIG. 9. Contrast experiment with silicon carbide revealing that $\underline{R} = 1/3[111]$.

FIG. 10. Direct lattice fringe image of the close packed planes in silicon carbide. Cubic regions (β) are intergrown with single polytype unit cells.

FIG. 11. An example of microsyntaxy in silicon carbide with faults F bordering the two polytypes.

FIG. 12. Rocking beam micro-diffraction of ~20Å regions on either side of a grain boundary, and from the grain boundary in mullite. (Courtesy of R. Geiss, IBM).

FIG. 13. High angle grain boundary between two α-silicon nitride grains revealed by direct lattice fringe imaging. Since the lattice fringes can be followed right up to the grain boundary from both sides, no intergranular amorphous layer exists.

FIG. 14. Another high angle grain boundary between two α-silicon nitride grains observed by direct lattice fringe imaging. The absence of any intergranular phase is again demonstrated by the lattice fringes running into the boundary. The unit cell high step (arrowed) is a common feature of the grain boundaries in silicon nitride.

XBB 7511 7641

FIG. 1

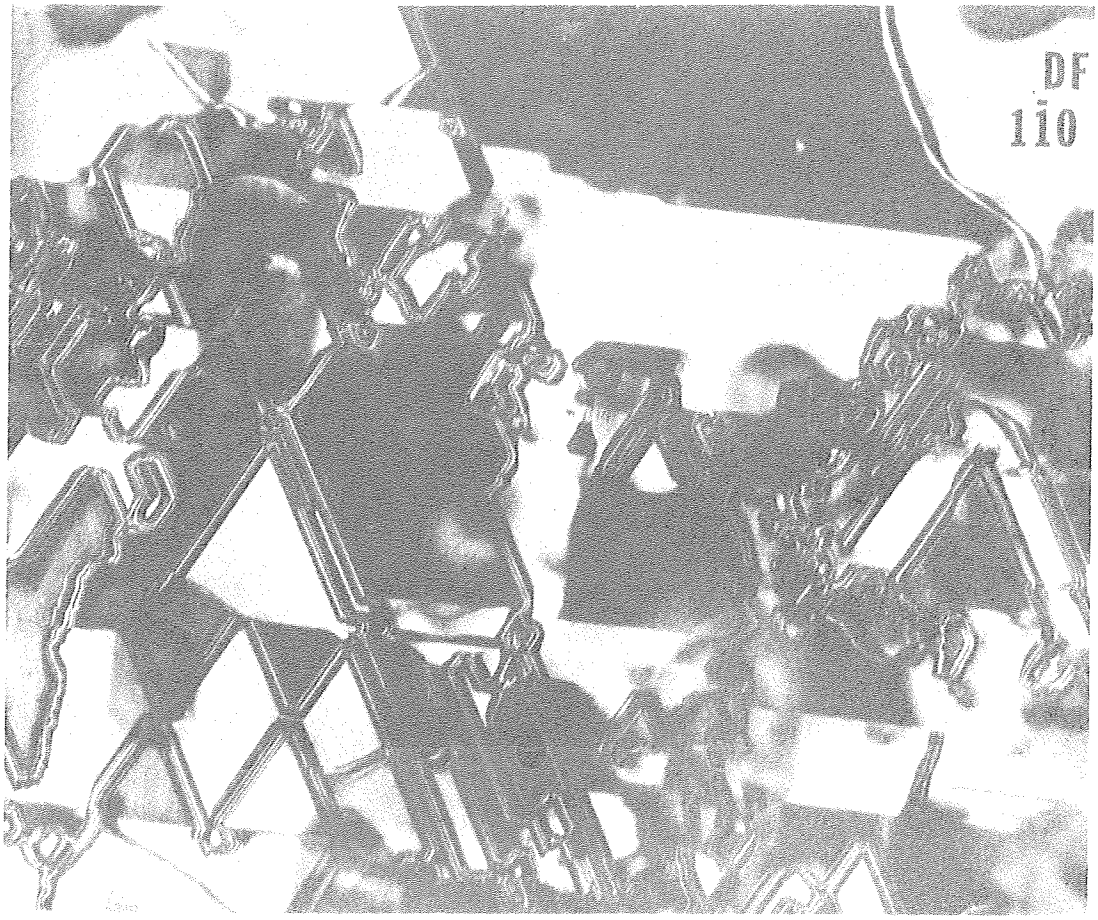

XBB 766 5394

FIG. 2

t=1.6s
t=4.0s
t=.8s
t=3.2s
t=0s
t=2.4s

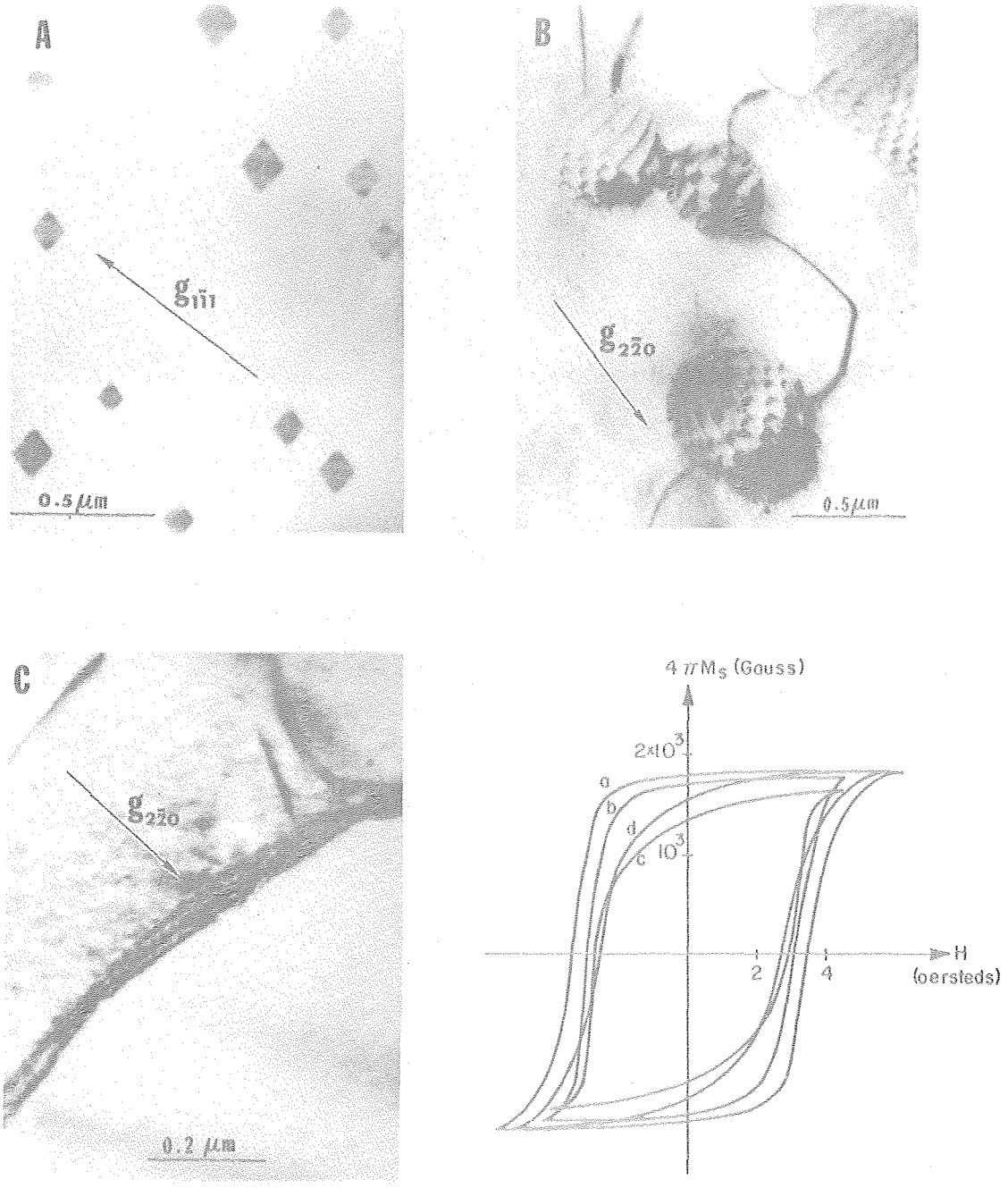

XBB 766 5125

FIG. 4

XBB 7511 8877

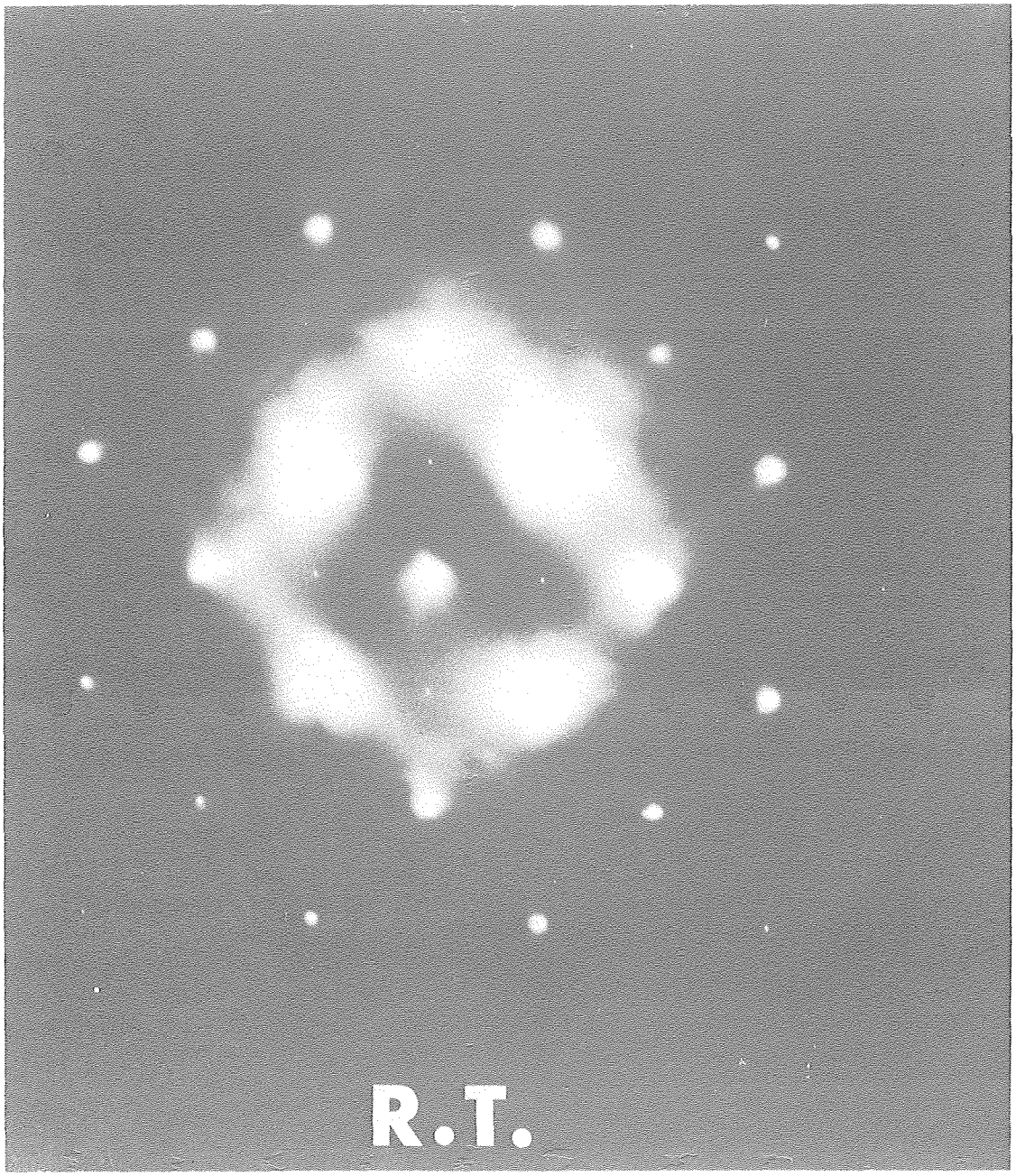

XBB 767 5947

FIG. 6a

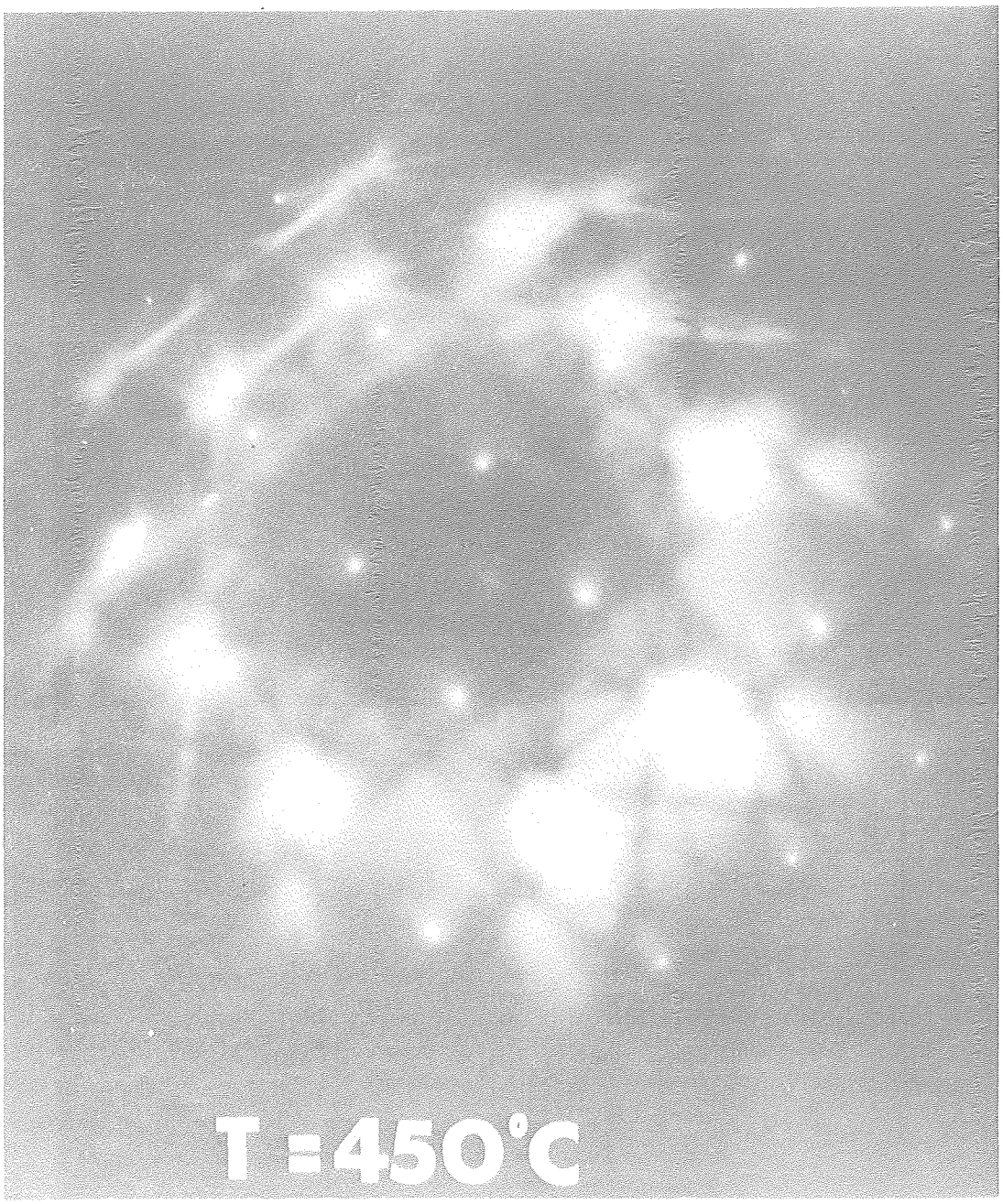

XBB 767 5946

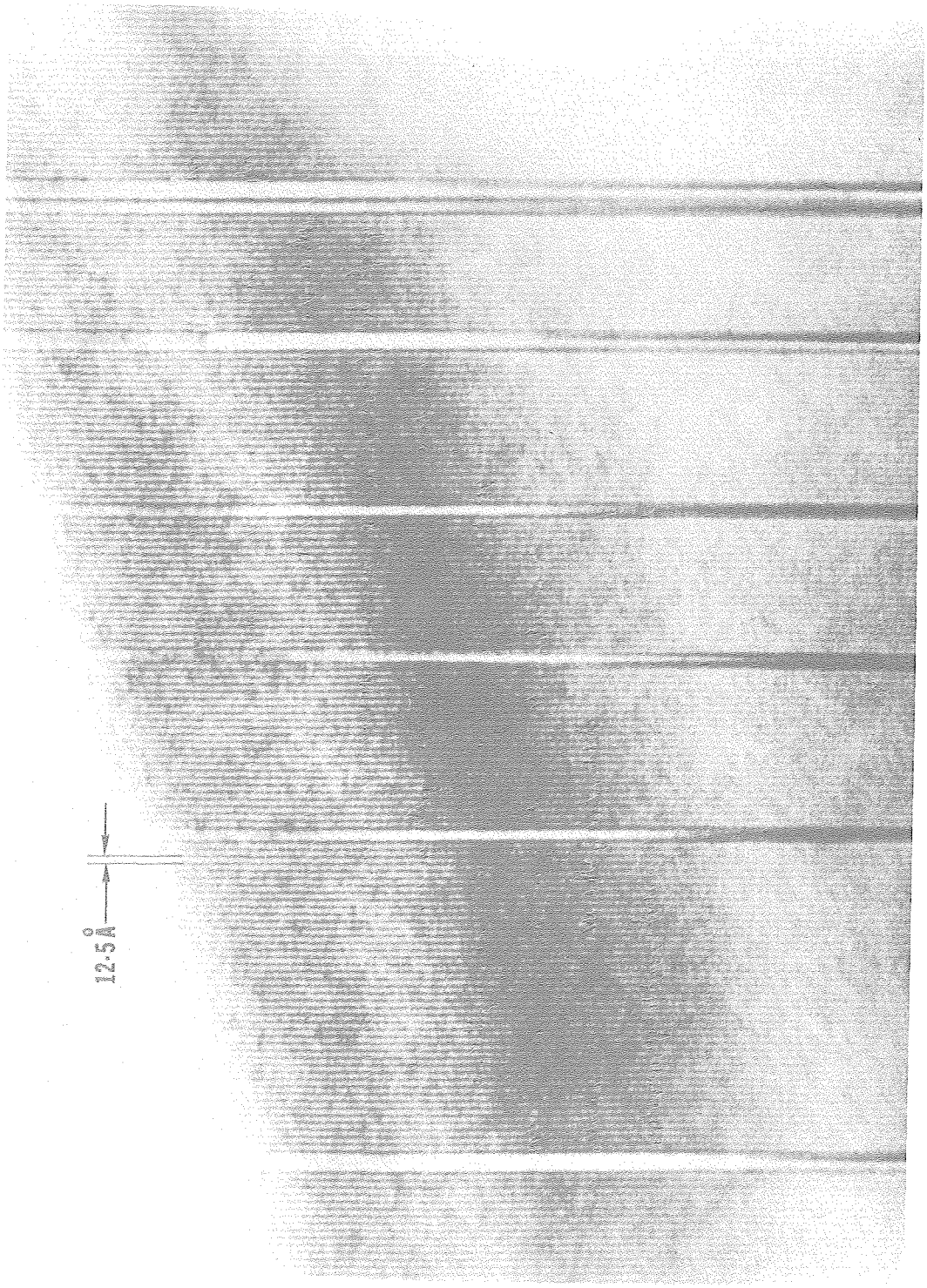

XBB 768 6819

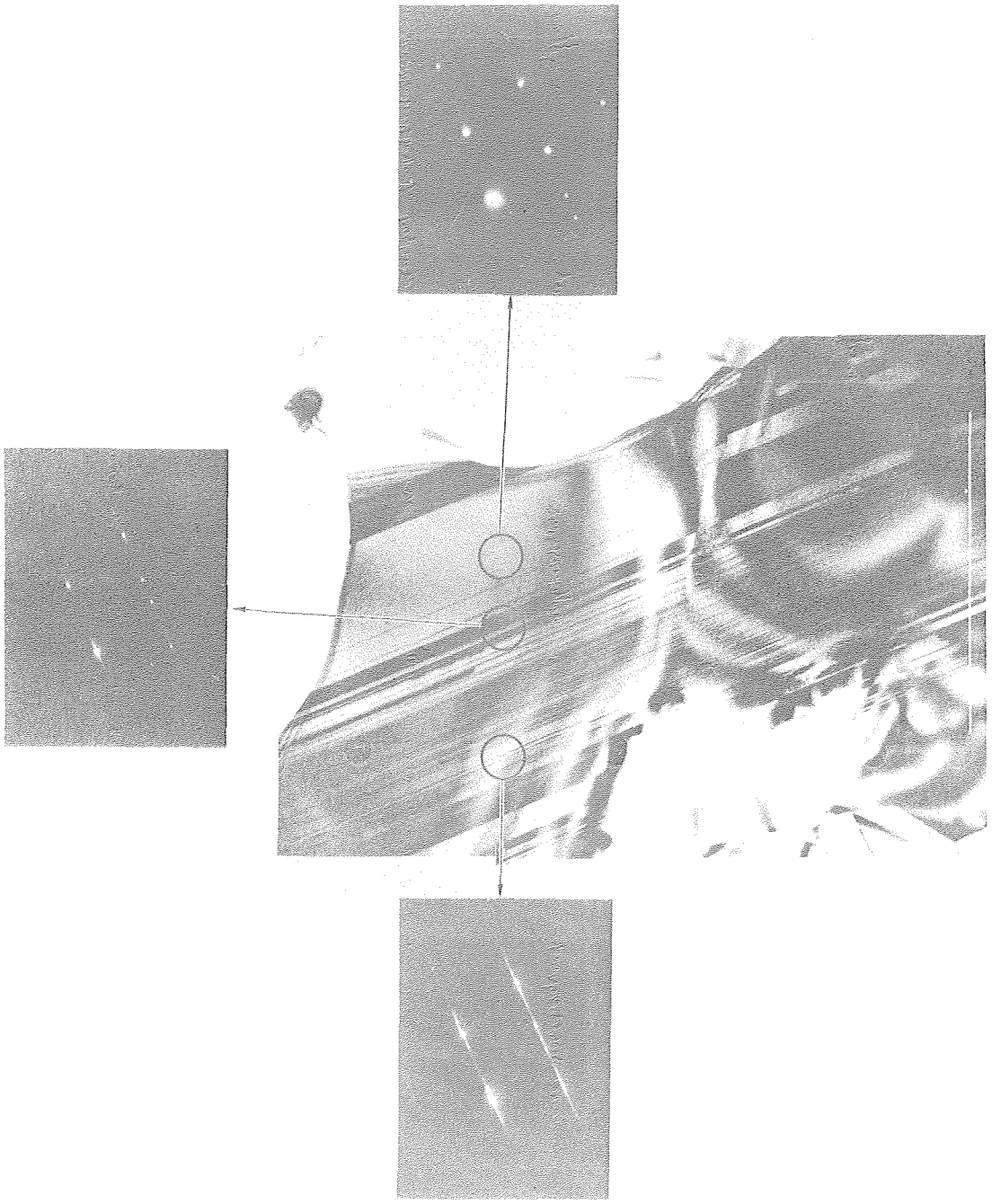

FIG. 8

XBB 769 8333

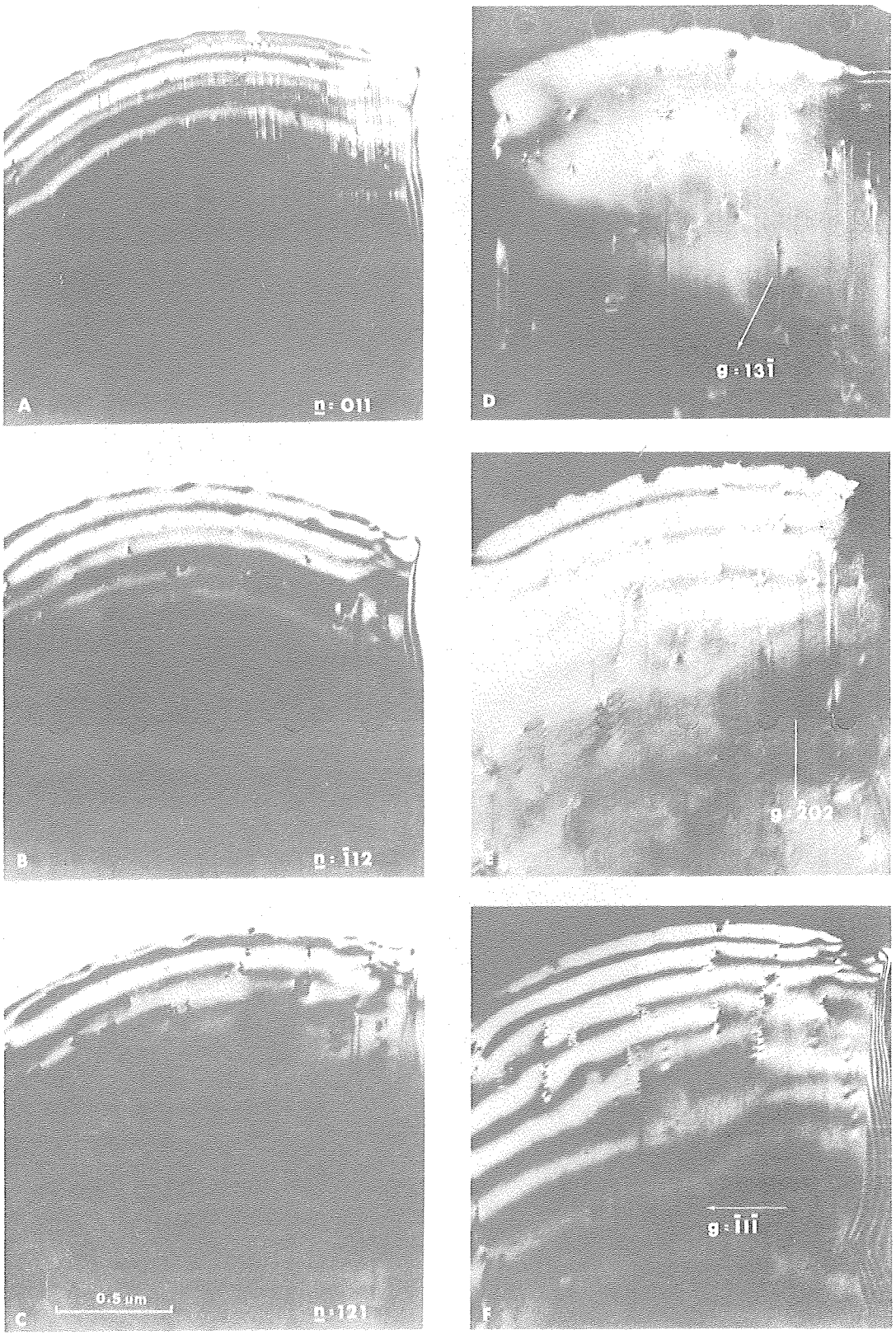

FIG. 9

XBB 767 6521

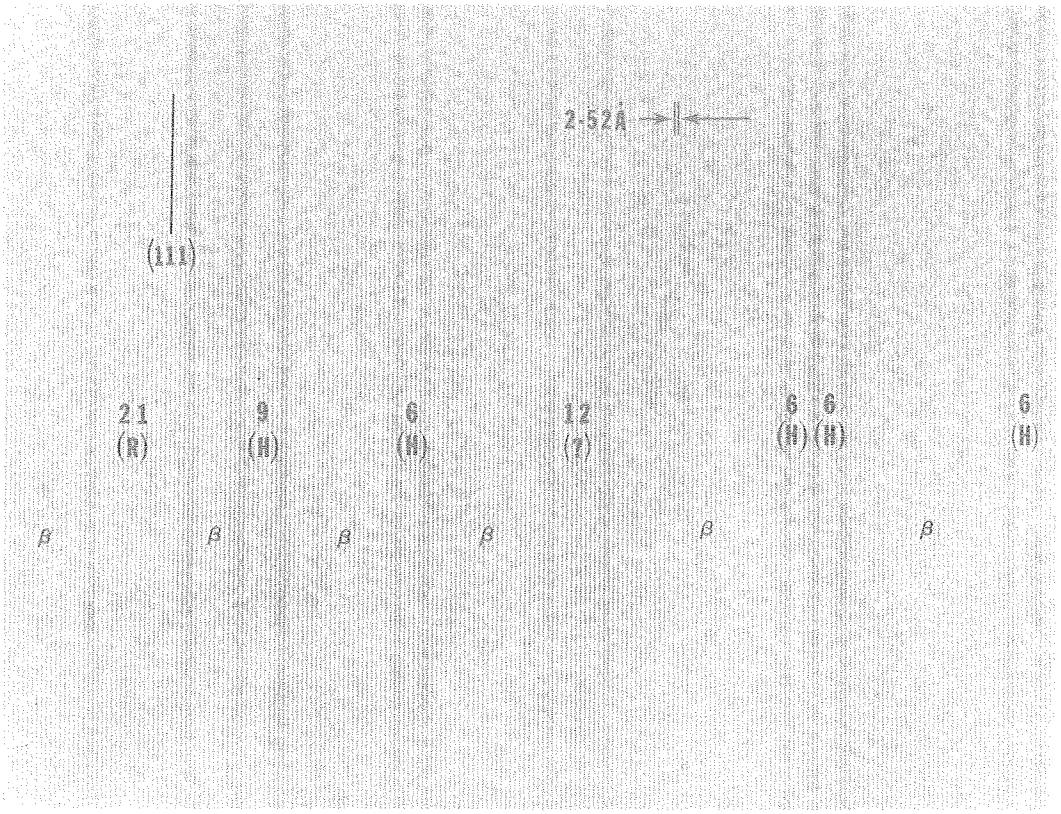

FIG. 10

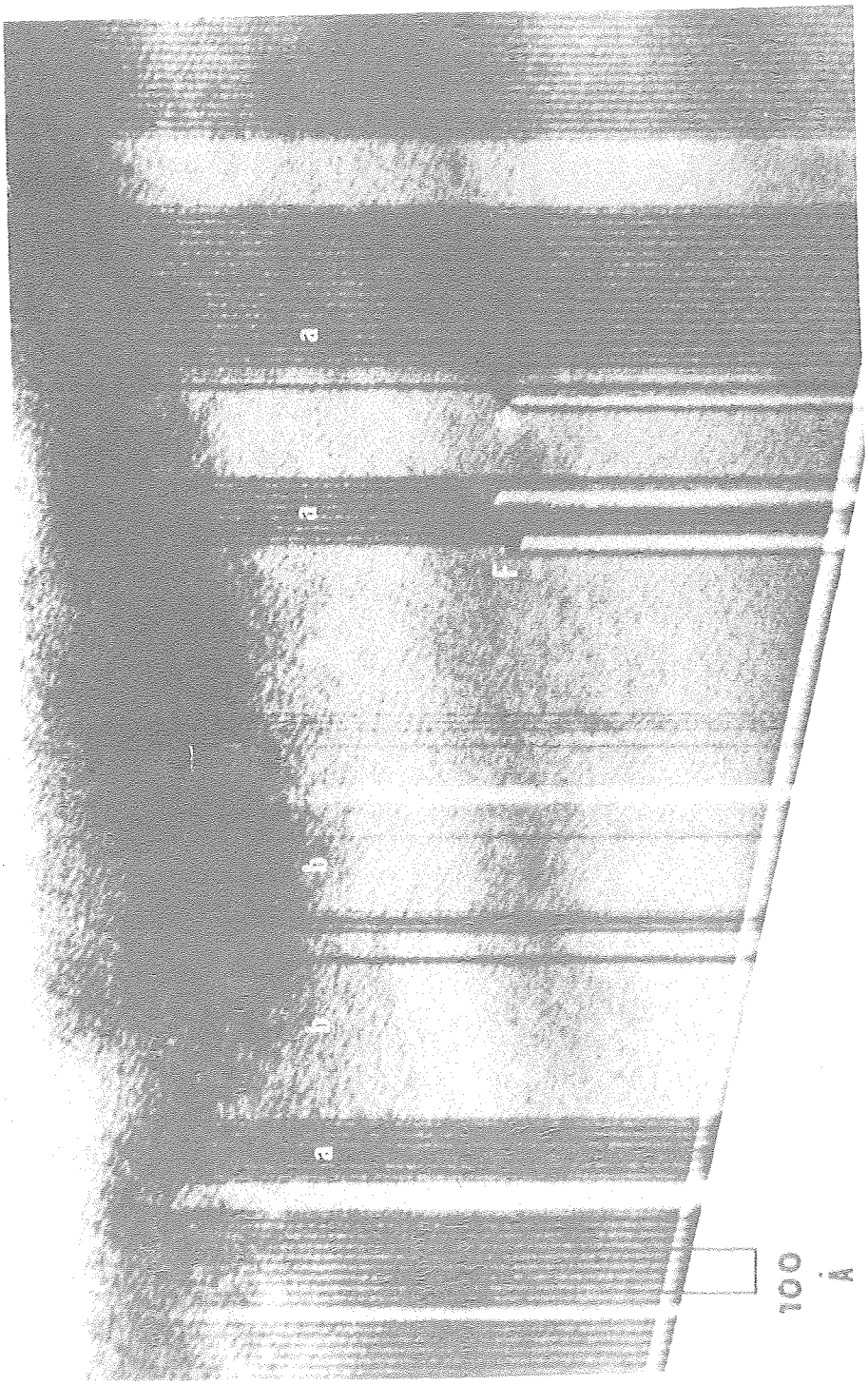

XBB 768 6520

FIG. 11

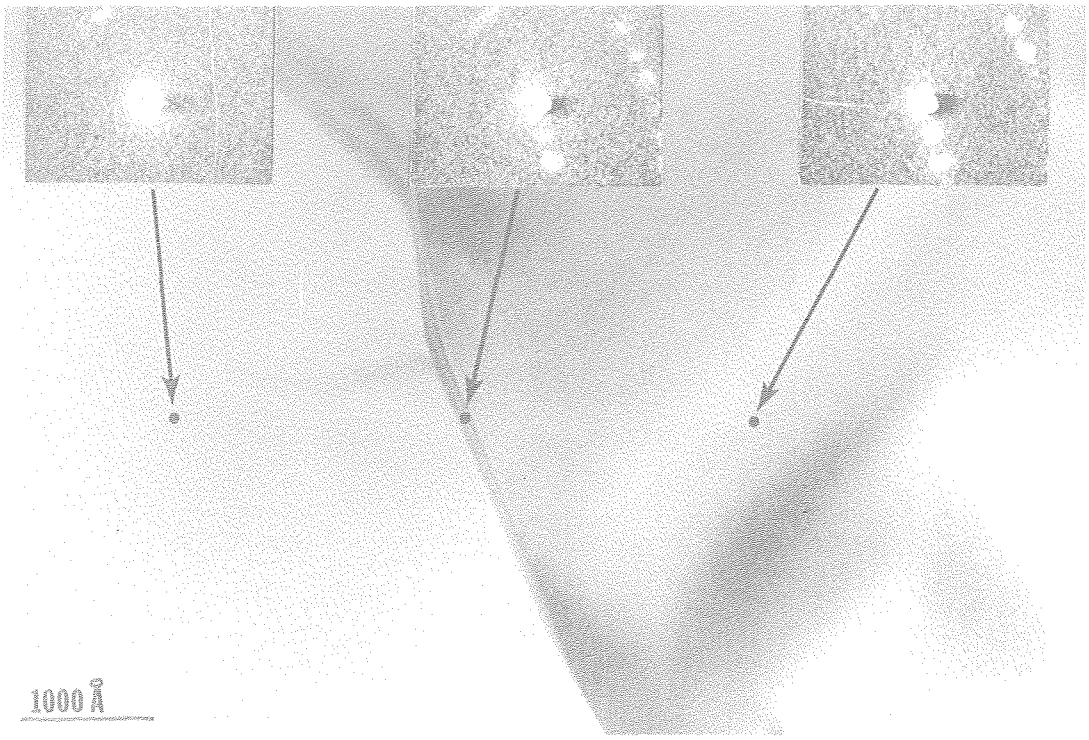

XBB 760 10011

FIG. 12

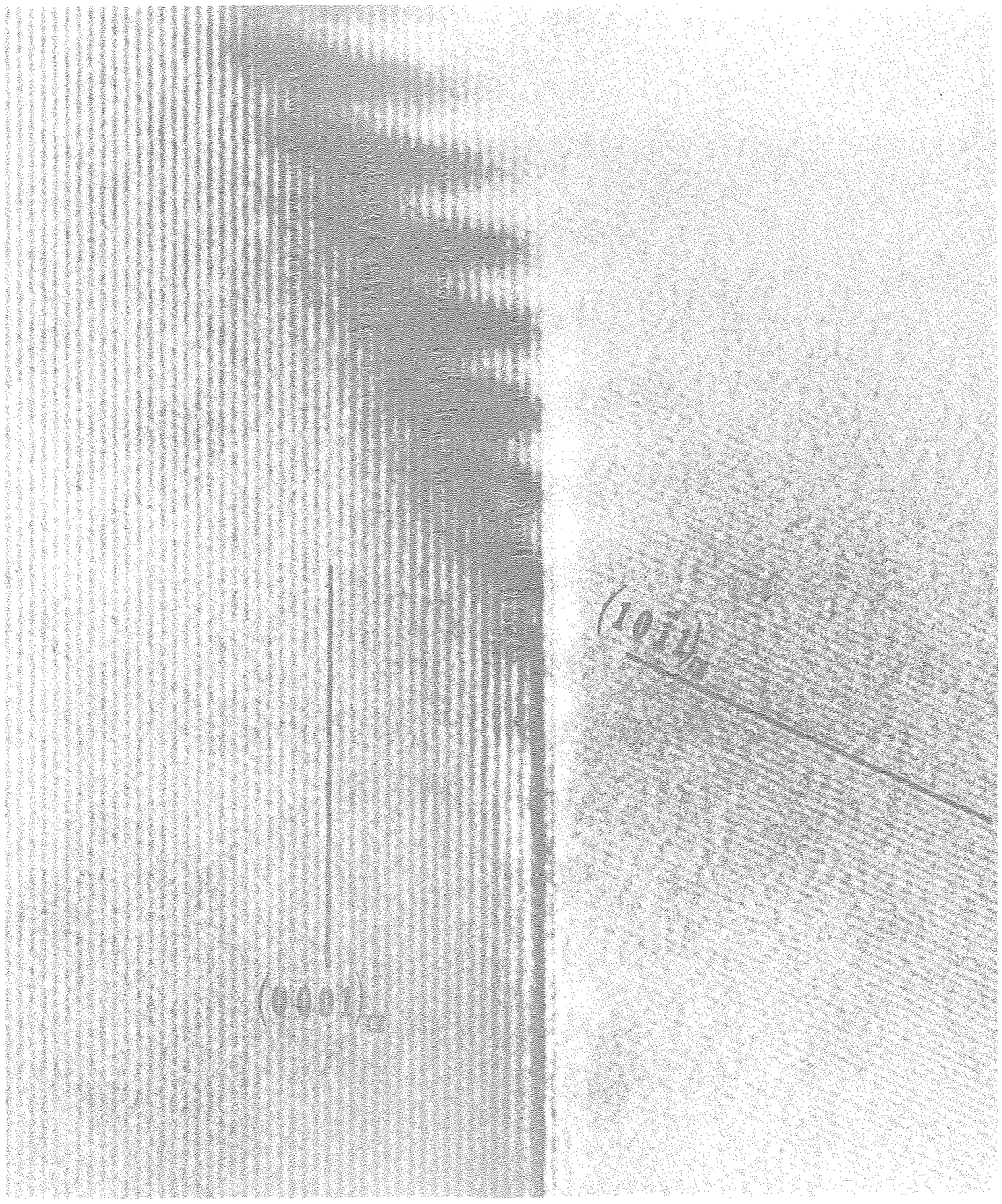

XBB 768 6448

FIG. 13

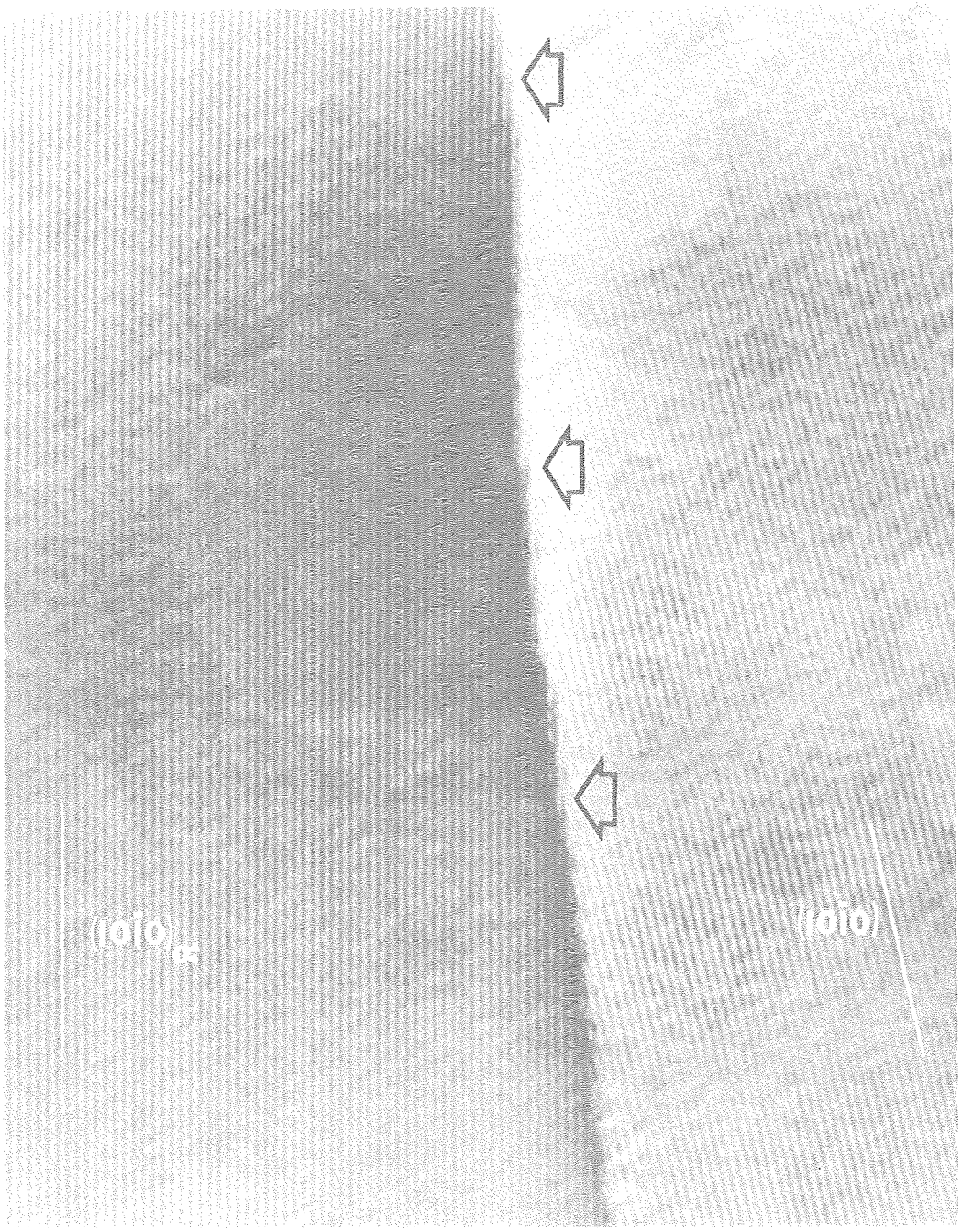

XBB 7610 9736

FIG. 14